

V. Naulin, W. Fundamenski, E. Havlíčková, Chr. Maszl, G. Xu, A.H. Nielsen,  
J. Juul Rasmussen, R. Schrittwieser, J. Horacek, J. Seidl  
and JET EFDA contributors

# Progress in Turbulence Modeling JET SOL and Edge Phenomena

“This document is intended for publication in the open literature. It is made available on the understanding that it may not be further circulated and extracts or references may not be published prior to publication of the original when applicable, or without the consent of the Publications Officer, EFDA, Culham Science Centre, Abingdon, Oxon, OX14 3DB, UK.”

“Enquiries about Copyright and reproduction should be addressed to the Publications Officer, EFDA, Culham Science Centre, Abingdon, Oxon, OX14 3DB, UK.”

The contents of this preprint and all other JET EFDA Preprints and Conference Papers are available to view online free at [www.iop.org/Jet](http://www.iop.org/Jet). This site has full search facilities and e-mail alert options. The diagrams contained within the PDFs on this site are hyperlinked from the year 1996 onwards.

# Progress in Turbulence Modeling JET SOL and Edge Phenomena

V. Naulin<sup>1</sup>, W. Fundamenski<sup>2</sup>, E. Havlíčková<sup>2</sup>, Chr. Maszl<sup>3</sup>, G. Xu<sup>4</sup>, A.H. Nielsen<sup>1</sup>,  
J. Juul Rasmussen<sup>1</sup>, R. Schrittwieser<sup>3</sup>, J. Horacek<sup>5</sup>, J. Seidl<sup>5</sup>  
and JET EFDA contributors\*

*JET-EFDA, Culham Science Centre, OX14 3DB, Abingdon, UK*

<sup>1</sup>*Association EURATOM- Risø DTU, Risø National Laboratory for Sustainable Energy, Technical  
University of Denmark, Bldg. 128, 4000 Roskilde, Denmark*

<sup>2</sup>*EURATOM-CCFE Fusion Association, Culham Science Centre, OX14 3DB, Abingdon, OXON, UK*

<sup>3</sup>*Association EURATOM/ÖAW, Institute for Ion Physics and Applied Physics,  
University of Innsbruck, Austria*

<sup>4</sup>*Institute of Plasma Physics, Chinese Academy of Sciences, Hefei 230031, People's Republic of China*

<sup>5</sup>*Association EURATOM-IPP.CR, Institute of Plasma Physics, Prague, Czech Republic*

*\* See annex of F. Romanelli et al, "Overview of JET Results",  
(23rd IAEA Fusion Energy Conference, Daejeon, Republic of Korea (2010)).*

Preprint of Paper to be submitted for publication in Proceedings of the  
23rd IAEA Fusion Energy Conference, Daejeon, Republic of Korea  
(10th October 2010 - 16th October 2010)



## **ABSTRACT**

Fluid turbulence modeling of the Scrape-Off Layer (SOL) has been an area of promising progress. Here we report on results obtained using codes that relax the usual scale separation paradigm in the SOL and treat fluctuations and time averaged background profiles simultaneous and without separating them.

Initial modeling is based on an interchange model of the SOL assuming that parallel effects appear in form of loss terms, estimated from assuming sheath limited situations or free expansion with ion sound speed along magnetic field lines depending on the connection length. Excellent progress has been achieved with the ESEL code [1] simulating the SOL of smaller devices. The higher temperature SOL of JET has still been modeled with good success [2]. Compared to the SOL of smaller devices the SOL of JET seems to exhibit more 3D effects which are not included in the 2D nature of the original code, which presumes the absence of drift waves in the edge, and - more importantly - uses plasma streaming off with ion sound speed in the parallel direction for the SOL. We have used several approaches to include these 3D effects.

## **1. PARALLEL LOSS TERMS**

Several authors have suggested that the parallel loss of polarization charge should scale with the Alfvén velocity [3]. A comparative investigation contrasting the dynamical consequences of both loss mechanisms rules out any model improvement with an Alfvén based loss term. We have investigated numerically parallel losses on the vorticity based on Alfvén velocity and ion sound speed intensively using the numerical code, ESEL, [1]. Using typical plasma parameters from the SOL the Alfvén velocity is 50–200 time larger than the ion sound speed, resulting in a very effective drain of momentum using Alfvén velocity to evaluate parallel losses. The number and strength of the observed blobs is therefore significantly smaller for simulations based on the Alfvén loss term compared to using ion sound speed. In figure 1, we show results obtained for both loss mechanisms. Using the ion sound speed for the losses we observe elongated blobs at the LCFS and circular blobs at the wall radius, in close agreement with observation from JET, see [4]. For losses occurring with the Alfvén speed in the simulation, we observe much lower amplitudes blobs which are also heavily damped. Further the blobs occurring in this kind of simulation have a circular shape already at the LFCS which changes to an elongated shape at the wall radius. Moreover the density profile in the SOL becomes completely flat. Neither of this does agree with observations [4], why we rule out the Alfvén speed based loss mechanism for SOL turbulence. More details on the simulation experiment comparison will be published in a forthcoming paper [5].

## **2. TRANSIENTS AND PARALLEL TRANSPORT**

To improve the accuracy of the modeled losses we therefore consider a one dimensional fluid model of the SOL based on Braginskii equations [6] (SOLF1D), which includes the interaction with neutrals. This model was adapted to cope with a fluctuating source prescribed by the perpendicular turbulent dynamics as modeled with ESEL, instead of the steady state source usually used to achieve stationary solutions.

A first comparison of the steady state loss terms showed that while the assumptions used in ESEL, namely Spitzer Harm diffusion and subsonic advection, seem to work well for the energy, the density loss time was off by an order of magnitude, specifically in the SOL including interaction with neutrals.

Figure 2 shows the response of the model to a short blob event. Two distinct velocities show themselves at  $t = 0.1\text{ms}$  (by increased plasma density production from neutrals) and  $t = 0.18\text{ms}$ , corresponding to electron thermal (conduction) and ion sound speed (convection). A non negligible reflection towards the outboard midplane at  $x = 0$  can be seen. Figure 3 shows parallel particle density and electron cooling times (left) compared to the approximation used in the ESEL code. The electron cooling time recovers faster to its initial value, while larger discrepancy is observed in the density. The scatterplot of the particle and thermal losses over density and temperature respectively (right) reveals a complex structure of the parallel losses in the one-dimensional fluid model (the approximation in ESEL is represented by linear dependence), while streaming off with ion sound speed is a dominating loss channel [7].

### 3. NON-GAUSSIAN INPUT TO THE 1D MODEL

The next step in coupling of the SOLF1D code with ESEL is investigating the plasma response in the SOL to a source that has a complex non Gaussian PDF. The source reflecting turbulent processes at the outboard midplane provided by ESEL was used with the aim to estimate the difference between the steady-state description of parallel transport in the SOL based on the use of time-averaged physical quantities and the fully time-dependent approach. In the model with fluctuations, the time average of complex quantities such as collisionality, differs significantly from the the same quantity calculated from the time averaged fundamental plasma parameters, temperature and density. Fluctuations are prescribed by the ESEL model at the outboard midplane ( $x = 0\text{ m}$ ) and evolve along the field line to the divertor target ( $x = 15\text{ m}$ ). The observed deviations increase with the amount of intermittency observed and are greatest in the far SOL and close to the target plates. Table 1 shows a selected overview of this effect and more results can be found in [7].

### 4. BLOB BIRTH IN JET SHEAR LAYER

We further investigated the occurrence of coherent structures in the SOL using JET probe measurements. These structures are originating on the mesoscale, with sizes much larger than the hybrid gyroradius lengthscale  $q_s$ . This scaling is consistent with order unity fluctuation levels at the edge. Moreover, even for low local values of the plasma beta the dynamics is essentially electromagnetic, and any imbalance in the parallel gradient force  $e n \partial_{\parallel} (\Psi - \phi)$  will allow a parallel current and thus magnetic perturbations to arise. The origin of blobs could be fixed to the edge shear region [5], by investigating the PDF of the density fluctuations measured by the reciprocating probe. It showed that the skewness of the PDF changes sign in the edge shear region, indicating positive density structures travelling outwards from that location and density depressions travelling inwards from the shear layer. Thus blobs appear to be generated paired with a density depletion – termed a hole. While the blobs propagate outward into the SOL the holes propagate inward to the edge

plasma in accordance with the interchange or curvature polarisation mechanism for blob charging and subsequent radial blob propagation. However, the lifetime of the holes, compared to the longer lived blobs, is limited due to the fast speed with which the edge plasma fills in the hole structure along magnetic field lines, a mechanism not active for the blobs propagating into the SOL.

## **5. PALMTREE MODE AS A SIGNATURE OF AN INWARD PROPAGATING HOLE**

Experimental observations show that ELMs lead to the ejection of blob-like current carrying filamentary structures into the SOL. In analogy to blob and hole like transport observed in tokamak turbulence, one can conjecture that also ELMs leave holes behind. The lifetime of these holes are in generally rather short and influenced by local shear, resistivity and therefore by the filling rate parallel to the magnetic field. If such a hole however is able to reach a resonant surface with a low rational  $q$ , it closes on itself and increases its lifetime significantly. We believe that the Palm Tree Mode (PTM) is a signature of such an event (Figure 3) [6].

Using in-vessel magnetic pick-up coils to reconstruct the PTM it is evident that the mode is highly localized. The PTM is a rather sharply bounded 1D filamentary structure on a 2D surface. It is therefore more reasonable to describe the PTM as a nonlinear coherent structure instead of by its Fourier components. We thus use the concepts of interchange turbulence driven blobs in an attempt to understand this mode.

In this picture the origin of the PTM is quite intuitive. As the ELM convects particles, energy and current out in filamentary structures, a hole in density with a corresponding current perturbation remains travels radially inwards from location of the ELM instability.

If large enough holes are arrested on resonant surfaces one can speculate that their lifetime will be enhanced and become large enough to be detected. A signature of such an event can be found in the so-called Palm Tree Mode (PTM) [8], which is unique to JET. We were able to identify this phenomenon as a decaying current filament hole on a magnetic resonant surface, originating after an ELM event. Fast sampling magnetic pickup coils were used to study the dynamics of the mode. Comparisons with Charge eXchange Recombination Spectroscopy (CXRS) were done to determine whether the frequency increase of the PTM is compatible with the recovery of edge plasma rotation after ELM induced momentum losses [9]. Further our investigations show that the maximum toroidal angular frequency of the mode is in good agreement with edge rotation after recovery. The PTM is therefore co-rotating with the ambient edge plasma. ECE was used to localize the PTM, which allowed estimation of the hole current. Two phases could be identified: initially a rapid loss of current was observed followed by a linear, much slower decay of the current. The first phase could be identified as diffusive transition phase from a peaked to a flat current distribution as the current filament is formed. A subsequent resistive linear decay phase is a strong indicator that the hole current filament is localized, closed and filled by perpendicular transport. This explains directly the many harmonics in the characteristic spectra and the long lifetime of the mode (up to 60ms).

In this contribution we focus on the events after the initial current perturbation has been created. As example a single PTM of Pulse No: 73568 in the time window  $t=12.98-13.02s$  was modelled. The redistribution of current observable at various positions in JET gives rise to the assumption

that an initially poloidally peaked current distribution spreads out and transforms into a uniform current distribution as the filament is formed.

$$\frac{\partial j}{\partial t} = D_{\parallel} \nabla_{\parallel}^2 j - \eta_{\parallel} \frac{e^2 n}{m_e} j \quad (1)$$

Neglecting perpendicular dynamics this behavior can be depicted by Eq. (1) where  $e$  designates the elementary charge,  $m_e$  the electron mass and  $n$  the plasma density. An initially peaked current density distribution  $j$  diffuses along a closed magnetic field line at a rate given by the parallel diffusion constant (Figure 4). The parametrization of a filament on a magnetic  $q=3$  surface is found by using EFIT.

Additionally current density is lost due to parallel Spitzer resistivity. Comparisons of the frequency increase of the PTM with CXRS show that the PTM is co-rotating with the edge plasma. The frequency increase of the investigated PTM is given by Eq. (2).

$$v_{tor} = 14.8 \cdot 10^3 + 9.2 \cdot 10^3 \cdot (1 - e^{-169 \cdot t}) \text{rad/s} \quad (2)$$

These results, together with the location of the probes in JET, were used as input parameters for Biot Savart's law to forward model the magnetic signature of a Palm Tree Mode guided by experimental results.

The obtained results (Fig.7) include all the features from the experimental results like the characteristic frequency increase, the different decay phases, and the many harmonics due to spatial localisation of the PTM.

In Figure 8 we show the filament and the distribution of the current in the filament 24 ms after the start of the simulation.

In summary we were therefore able to find a simple and intuitive method to describe complex current structures in the pedestal of JET. The PTM therefore gives valuable insight into ELM physics. Implications on ELM physics should be discussed in the future.

## CONCLUSION

Our work shows that the concept of blobs and holes is not only useful to study turbulence and zonal-flow generation, but it is also important and applicable to macroscopic structures like ELMs and PTMs. Using numerical simulations the Alfvén mechanism for SOL losses was ruled out to be important for blob propagation. Further increasing the level of parallel modelling used for outboard midplane turbulence simulations, the conductive/convective parallel dynamics were recovered in time-dependent 1D modelling, moreover the influence of skewed, non-Gaussian fluctuations of the basic plasma quantities on calculating complex parameters important in the SOL dynamics was shown. Specifically for the far SOL and close to the divertor targets, a large impact of the fluctuation characteristics on these quantities was shown. This can be a missing ingredient in current SOL modelling.

As for the blob structures responsible for the SOL intermittency we could conclusively show that their origin is located at the maximum shear in the L mode edge shear layer. Furthermore blobs

and holes are generated simultaneously. A similar generation of holes was conjectured for ELMs where the presumed hole can be arrested on a low rational flux surface. We believe that the PTM is such a hole structure, showing that the ELM starts localised at the outboard midplane and with a finite perturbation in the plasma current. Thus critical insight into mechanisms for intermittent edge and SOL transport was found, all of which will enter SOL transport modelling and improve our ability to improve the predictions for ITER SOL profiles and heat loads, with the prospect that further clarifying the composition of the ELM structure will help putting control schemes on a firmer theoretical basis.

## ACKNOWLEDGEMENTS

This work was supported by EURATOM and carried out within the framework of the European Fusion Development Agreement. The views and opinions expressed herein do not necessarily reflect those of the European Commission.

## REFERENCES

- [1]. O.E. Garcia et al., Physical Review Letters, **92**, 165003 (2004); O.E. Garcia, R. A. Pitts, J. Horacek, et al., Plasma Physics and Controlled Fusion **49**, B47 (2007)
- [2]. Naulin et al., Proc. 21st IAEA Fusion Energy Conference, Chengdu, China (2006); Fundamenski Nuclear Fusion **47** (2007) 417-433
- [3]. B.D. Scott, private communication,
- [4]. G.S. Xu et al., Nuclear Fusion 49, 092002 (2009); G.Huysmanns et al. IAEA 2010
- [5]. A. H. Nielsen et al., in preparation
- [6]. E. Havlíčková, Ph.D. thesis, Charles University, Prague (2009)
- [7]. E. Havlíčková et al., PSI 2010, to be published in Journal of Nuclear Matterials.
- [8]. H. Koslowski et al., Nuclear Fusion **47**, 201 (2005)
- [9]. T. W. Versloot et al., Plasma Physics and Controlled Fusion **52**, 045014 (2010)

	$x = 0\text{m}$	$x = 10\text{m}$	$x = 14.95\text{m}$	$x = 15\text{m}$
steady-state value				
$n_s [10^{19} \text{ m}^{-3}]$	2.05	2.51	9.12	0.84
$T_s [\text{eV}]$	20.99	16.56	3.19	1.92
average value				
$\langle n \rangle [10^{19} \text{ m}^{-3}]$	2.05	2.40	7.73	1.35
$\langle T_e \rangle [\text{eV}]$	20.99	20.33	4.82	3.52
fluctuation level				
$\langle (n - \langle n \rangle)^2 \rangle^{1/2} / \langle n \rangle$	0.37	0.08	0.12	0.18
$\langle (T_e - \langle T_e \rangle)^2 \rangle^{1/2} / \langle T_e \rangle$	0.50	0.11	0.20	0.29
effect of averaging $\langle f(n, T_e) \rangle / f(n_s, T_s)$				
$f = nT_e$	1.18	1.17	1.27	3.03
$f = nT_e^{3/2}$	1.37	1.31	1.58	4.30
$f = T_e^{5/2}$	1.49	1.71	3.02	5.29
$f = T_e^{7/2}$	2.33	2.16	5.08	12.30
$f = n \overline{\sigma v}_{ion}$	1.04	1.23	5.35	117.33
$f = n \overline{\sigma v}_{cx}$	1.05	1.02	0.98	1.90
$f = n^2 \overline{\sigma v}_{rec}$	1.04	0.75	0.48	1.24
$f = n \overline{\sigma v}_{exc}$	0.98	1.06	2.53	21.39

Table 1: Inaccuracy in calculation of parallel transport parameters along the magnetic field introduced by averaging of the midplane density and temperature calculated as ratios of time-averaged and steady-state solutions.

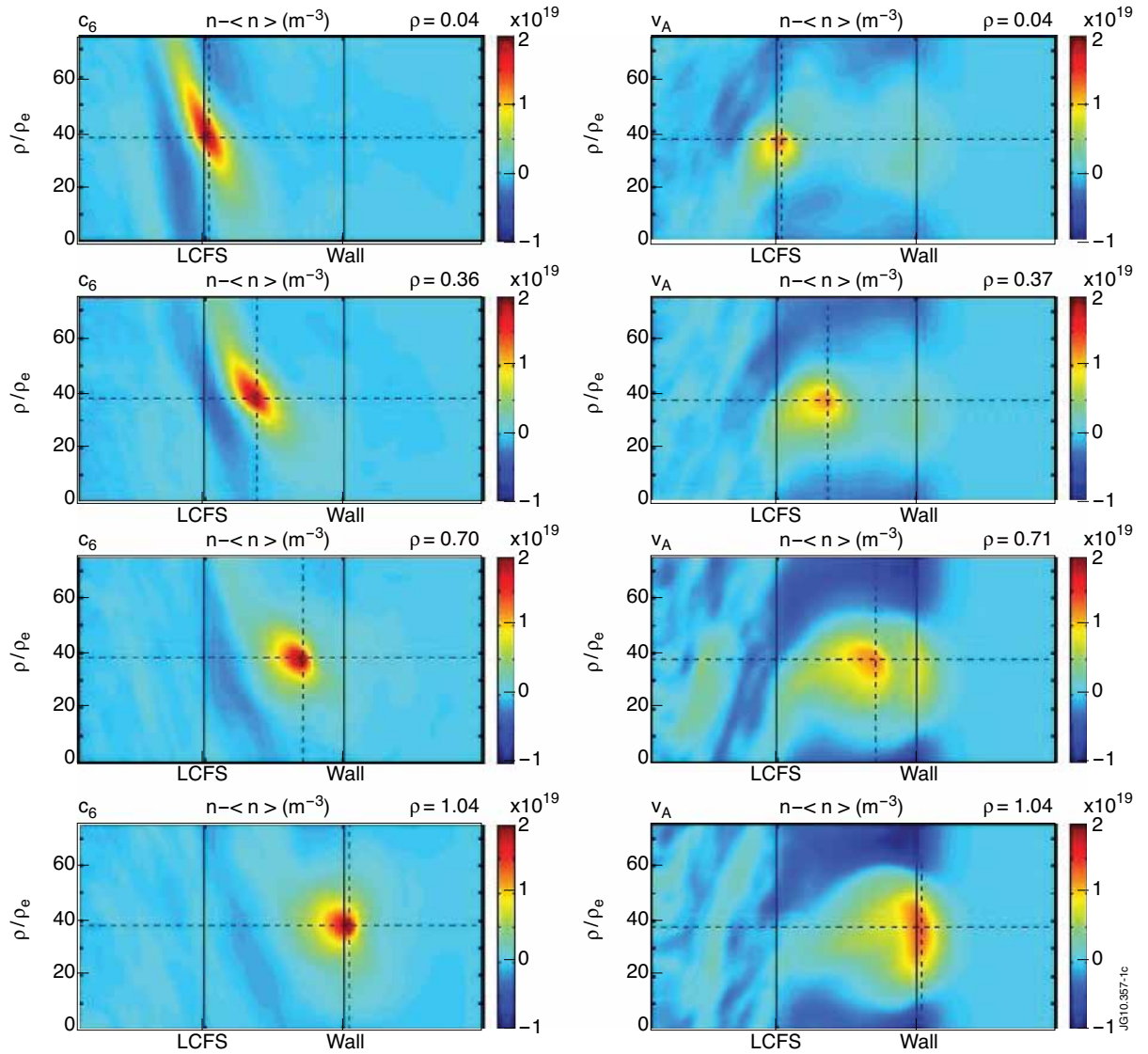


Figure 1: Conditional average density signal,  $n$  RMS=2, showing the full 2D domain, at 4 different radial positions located in the SOL. Loss by ion sound speed left side and by Alfvén speed.

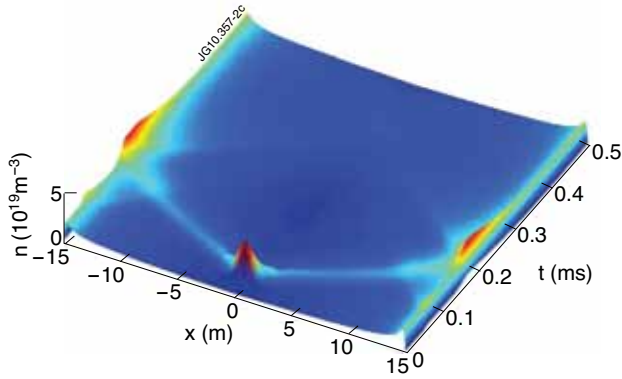


Figure 2: Density over time with blob as initial condition in SOLF1D.

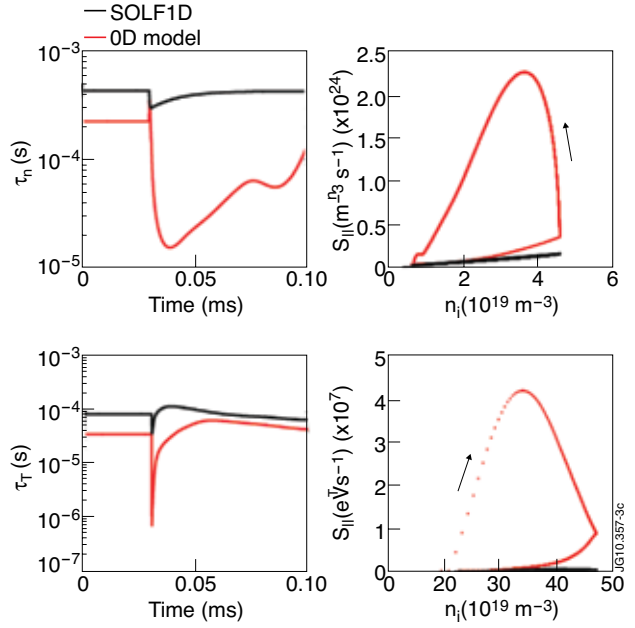


Figure 3: Parallel loss times  $\tau$  for density and temperature during a transient event and total parallel losses  $S_{\parallel}$  as functions of density and temperature. Comparison of SOLF1D solution and a simple approximation.

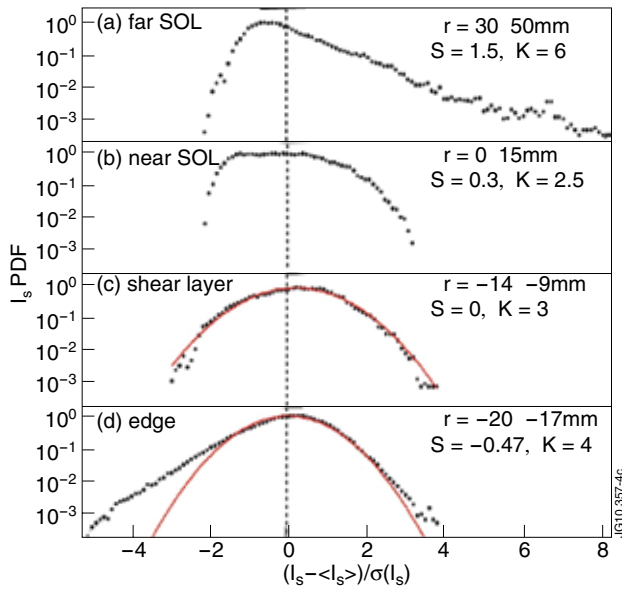


Figure 4: Density PDF at various positions with respect to the last closed flux surface.

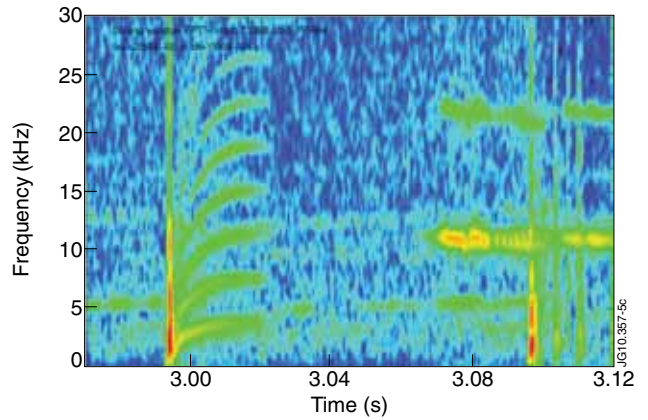


Figure 5: Spectrogram of the signal from a magnetic pickup coil at the outboard limiter of JET (JET Pulse No: 73568). The characteristic pattern inspired the name.

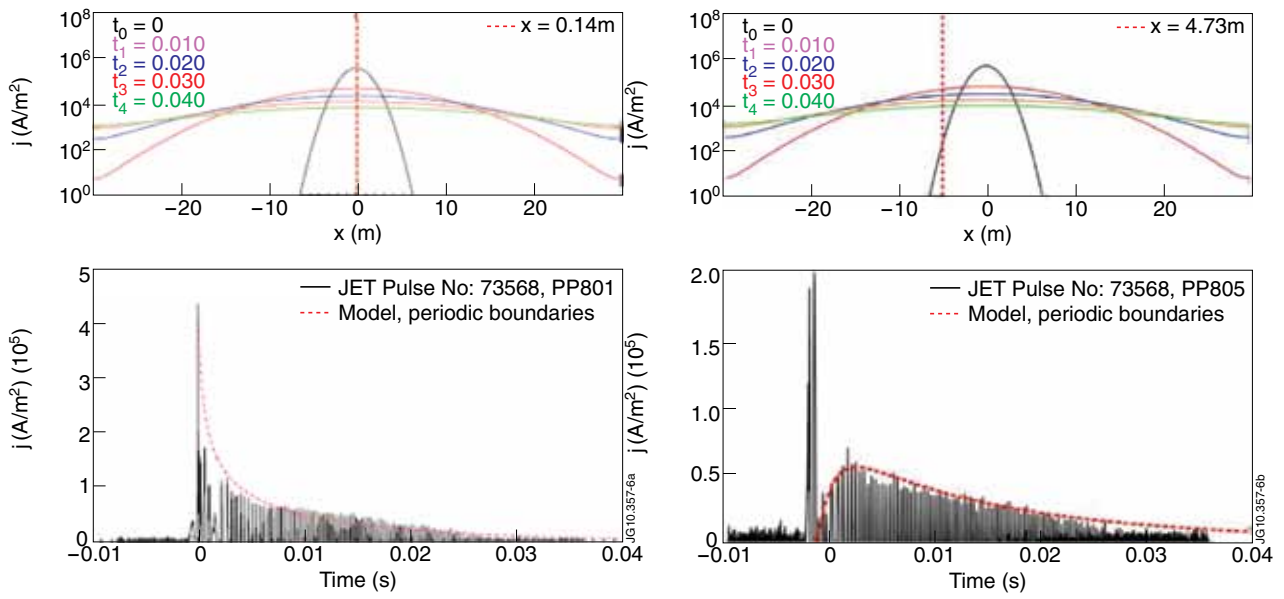


Figure 6: Comparison of measured and simulated current densities for two locations at the outboard limiter (JET Pulse No: 73568,  $t_0 = 12.9936s$ )

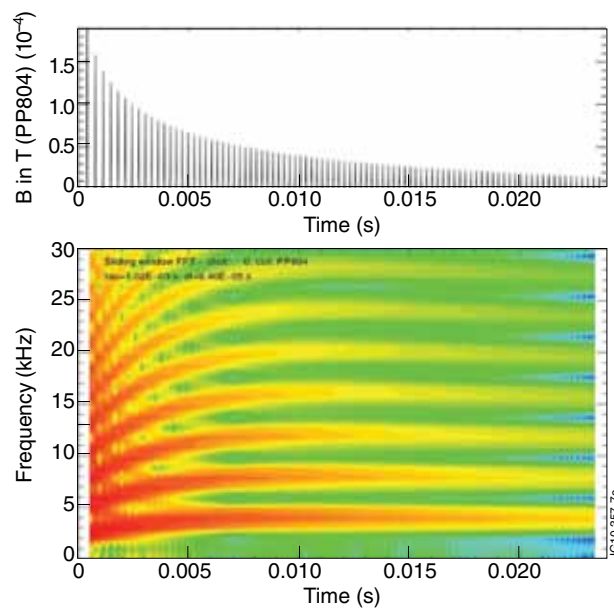


Figure 7: The obtained results by forward modeling are in a good agreement with the measured in Fig. 3.

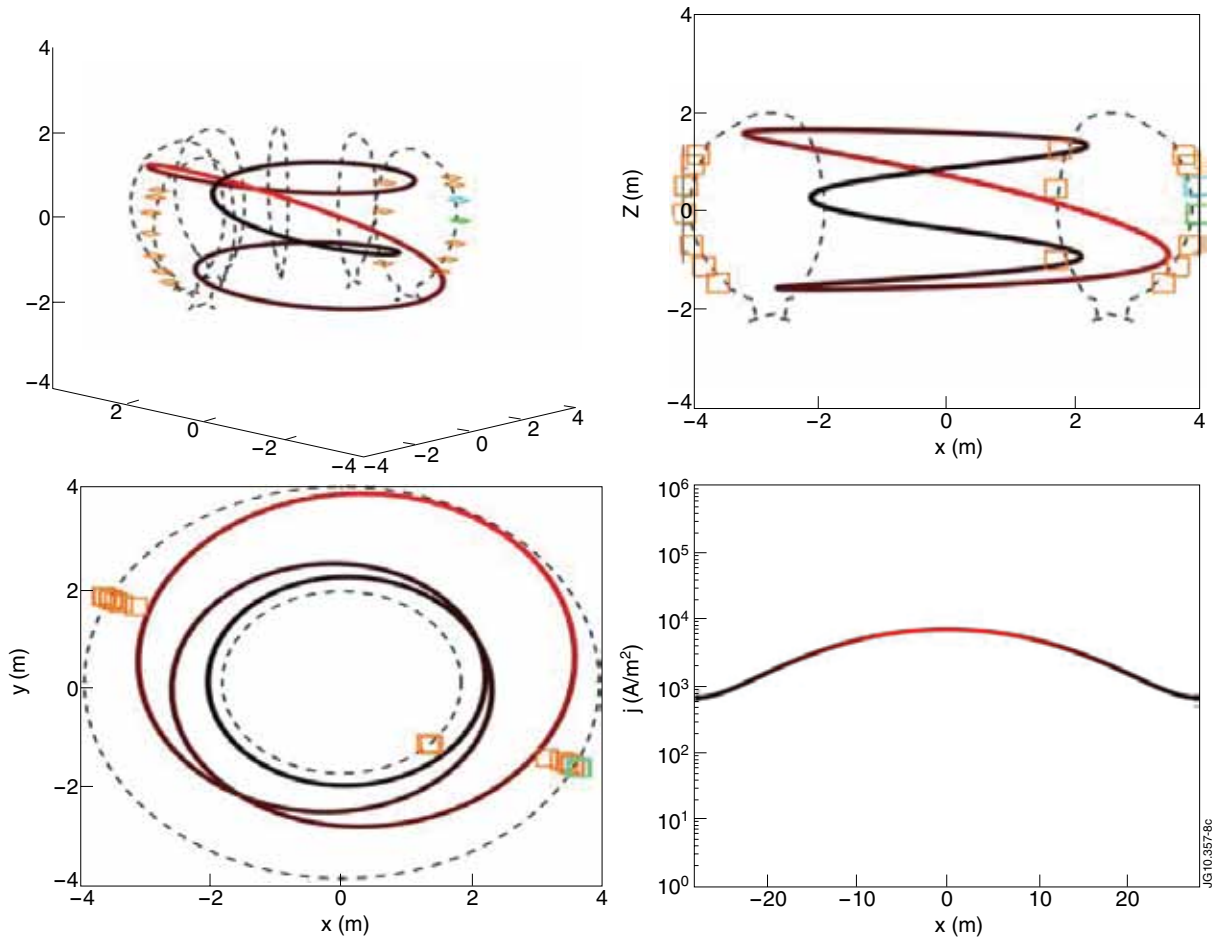


Figure 8: Redistribution of current density in the PTM filament after 24 ms